RPE | Radiation Physics & Engineering
An International Peer-Reviewed Journal
Published by K.N. Toosi University of Technology
http://rpe.kntu.ac.ir
Research Article

Radiation Physics and Engineering 2022; 3(2):1–6
https://doi.org/10.22034/RPE.2022.339003.1080

Two-dimensional modeling of atmospheric-pressure cold plasma jet generator for treatment application

Yasaman Amiri*, Behjat Ghasemi, Zahra Shahbazi Rad
Radiation Application Department, Faculty of Nuclear Engineering, Shahid Beheshti University, Tehran, Iran

HIGHLIGHTS

- The modeling of the plasma jet is performed for a constant voltage and frequency of 4.5 kV and 25 kHz, respectively.
- The jet device consists of two electrodes, a central pin electrode and a ring electrode, both made up of copper.
- Plasma parameters of electron density distribution, temperature distribution, and electric potential were calculated.
- The results showed that the electron density value was suitable for the therapeutic applications.

ABSTRACT

In this study, cold atmospheric pressure plasma jets for treatment application was studied with COMSOL Multiphysics by a finite element solver. The device operated with argon gas in atmospheric pressure which was supplied by an alternating current power supply. Effective plasma parameters for treatment such as electron density and temperature as well as electrical potential were investigated. Plasma parameters that affect treatment were determined by establishing a virtual laboratory before the experiment. Using this virtual laboratory, the plasma parameters with probable effects on the treatment can be determined before the experiment. The results showed that the electron density value was suitable for the therapeutic applications and the plasma temperature was in the allowable range for treatment.

KEYWORDS

DBD jet generation
Two-dimensional simulation
Cold plasma
Atmospheric pressure
COMSOL Multiphysics

HISTORY

Received: 24 April 2022
Revised: 30 April 2022
Accepted: 1 May 2022
Published: Spring 2022

1 Introduction

Cold plasma jets created in atmospheric pressure discharges are a fast-evolving technology (Fridman et al., 2008). Low gas temperature, high reactive chemical species, and easy plasma dynamics control have made cold plasma jets as an appropriate choice for a variety of essential industrial applications (Fridman et al., 2008). Neutral gasses that turn into ions create a conducive environment. The Coulomb interaction between the charged particles, which determines the gas dynamics, is one of the most important features of the ionized gasses (Chu et al., 2002).The Coulomb interactions between charged particles that determine the gas dynamics can be regarded as one of the most important features of ionized gasses. There are two categories of the ionized gasses: strongly- and weakly-ionized gasses. The Weakly-ionized gasses are those using a small fraction of charged particles, and their behavior is generally ruled by the neutral gas. However, the analysis of strongly ionized environments requires the electrodynamics rules to appropriately define such environments. The plasma physics in some specific applications is developed such as light sources, current shut-offs, thermal core fusion, plasma accelerators, nanotechnology, and plasma acupuncture (Lu et al., 2019).

In recent years, a wide range of plasma sources has been introduced with different names for biomedical applications. These include plasma needles, different dielectric barrier discharges (DBD), atmospheric pressure radiant discharge torches, plasma torches, plasma jets, and others. However, there are generally three commonly-used industrial plasma sources for biomedical applications: DBD, plasma jets, and radiant discharges.

Current studies mostly focus on DBDs and plasma jets. For example, Yan et al. (2016) (Yan et al., 2017) showed that out of all cancer treatment modalities that use cold atmospheric pressure plasmas, around 72% are based on plasma jets, about 21% on DBDs, and the remaining (i.e.,

*Corresponding author: y.amiri@mail.sbu.ac.ir

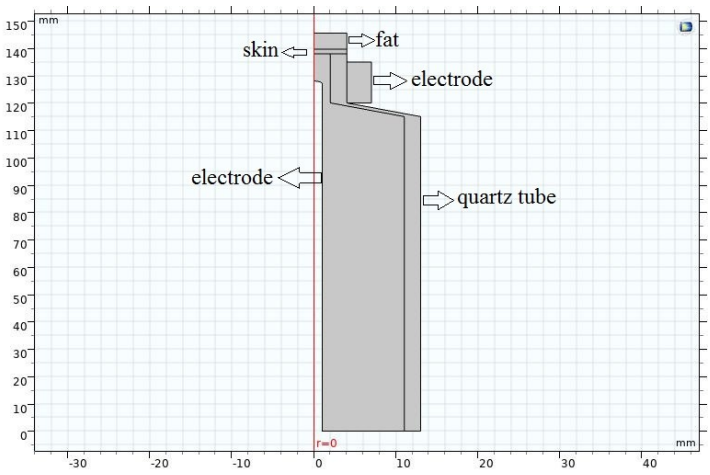

Figure 1: DBD jet and tissue configuration.

about 7%) on different devices.

Deepak et al. (Deepak et al., 2018) analyzed the electric specifications of a plasma jet DBD device that operates in atmospheric pressure with Argon gas. They used the plasma and fluid dynamics modules of COMSOL software (COMSOL, 2018) for plasma jet modeling.

This research aims to analyze plasma parameters values such as electron density, electron temperature, and electric potential for different alongside electric parameters changes, such as operating voltage and frequency. This study suggests that plasma parameters (i.e., electron density, electron temperature, and electric potential) increase as operational voltage and frequency values increase.

Sohbatzadeh et al. (Sohbatzadeh and Soltani, 2018) simulated one-dimensional DBD in 2018, where they measured various plasma parameters such as electron density, gas temperature, and other species. The alternating power supply worked in a maximum applied voltage of 30 kV and a frequency of 27 kHz. Sharma et al. (Sharma et al., 2020) created a model of a plasma jet DBD device which used argon gas with the DC pulse power supply. They determined different parameters such as plasma density, gas velocity distribution, and electric field distribution using COMSOL software.

Few simulations have been performed on atmospheric pressure jet based on DBD plasma so far. In this research, COMSOL Multiphysics was used to perform two-dimensional simulation of DBD atmospheric pressure plasma jet. Electron density and plasma temperature are two important parameters for treatment application that should be determined. So, these parameters were investigated as a case study. The low temperature plasma sources described above produce chemically reactive species including reactive oxygen species (ROS) and reactive nitrogen species (RNS), which are known from redox biology to play important biological roles (Lu et al., 2016). Other agents generated by these plasma sources are also suspected to play active roles in biological applications. These include charges particles (electrons and ions), UV and VUV radiation, and electric elds. For example the electric eld can cause electroporation of cell membranes, allowing molecules (including ROS and RNS) to enter the cells and cause damage to the cell's internal organelles (including mitochondria) and macromolecules such as lipids, proteins, and DNAs (Kogelschatz et al., 1997). There are some related researches in the refrences (Schröder et al., 2015; Mazandarani et al., 2020).

2 Materials and Methods

The modeling of the plasma jet is performed for a constant voltage and frequency of 4.5 kV and 25 kHz, respectively. The gas inside the jet is considered argon and the flow rate is 5 slm. Initial values for the electron density, the gas pressure, and the gas temperature are assumed to be 10^6 m^{-3}, 1 atm, and 300 K, respectively. These values indicated that the device is being operated in glow discharge region without any arcing phenomenon which is necessary for using a cold plasma jet in biomedical as well as technological applications (Raizer and Allen, 1991).The reduced electron mobility and corresponding energy were obtained using BOLSIG+ (Hagelaar and Pitchford, 2005).

It should be noted that, the reduced electron mobility and corresponding energy were obtained using BOLSIG+. In the following, the calculated plasma parameters are presented and discussed.

2.1 Geometry definition

The geometrical details for the DBD plasma jet generation are shown in Fig. 1. The main body of the jet consists of a quartz tube, and the inlet of the quartz tube and the working gas of the device is argon gas. The jet device consists of two electrodes, a central pin electrode, and a ring electrode, both of them made up of copper. The pin and the ring electrodes have been set as the powered electrode and the ground electrode, respectively. Tissue including skin and fat has been considered to be located at the output of the device and at the top of the plasma device as seen in Fig. 1.

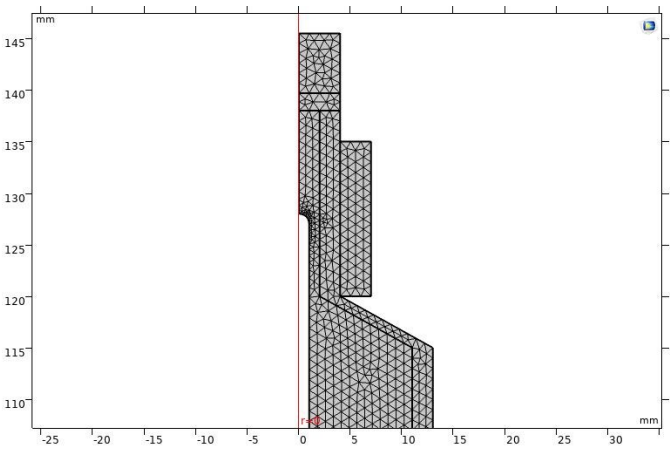

Figure 2: Meshing of DBD plasma jet using finite-element method (FEM).

2.2 The key equations for the simulations The essential equations for the modeling

The electron density and mean electron energy have been calculated by solving a pair of drift-diffusion equations for the electron density and mean electron energy as follows in Eqs. (1) and (2) (Hagelaar and Pitchford, 2005):

$$\frac{\partial}{\partial t}(n_e) + \nabla.[-n_e(\mu_e.E) - D_e.\nabla n_e] = R_e \tag{1}$$

$$\frac{\partial}{\partial t}(n_\varepsilon) + \nabla.[-n_\varepsilon(\mu_\varepsilon.E) - D_\varepsilon.\nabla n_\varepsilon] + E.\Gamma_e = R_\varepsilon \tag{2}$$

$$\begin{aligned} D_e &= \mu_e T_e \\ \mu_\varepsilon &= (\frac{5}{3})\mu_e \\ D_\varepsilon &= \mu_e T_e \end{aligned} \tag{3}$$

The source coefficients in Eq. (3) are determined by plasma chemistry using the rate coefficients (Mazandarani et al., 2020).

Electrons are lost to the wall due to random motion within a few mean free paths of the wall and gained due to secondary emission effects, resulting in the following boundary condition for the electron flux (Hagelaar and Pitchford, 2005):

$$-n\Gamma_e = \big((\frac{1}{2})\nu_e\big)n_e - \sum_p \gamma_p(\Gamma_p n) \tag{4}$$

and electron energy flux is calculated as:

$$-n\Gamma_\varepsilon = \big((\frac{5}{6})\nu_e\big)n_\varepsilon - \sum_p \varepsilon_p\gamma_p(\Gamma_p n) \tag{5}$$

where γ_p is the secondary emission coefficient and ε_p is the mean energy of the secondary electrons. At the walls, argon metastable quench and change back to neutral argon atoms. Argon ions also change back to neutral argon atoms while emitting secondary electrons.

Governing equations describing the fluid theory originate from solving a set of moments of the Boltzmann equation. Typically, for most applications, only the first three moments (i.e., particle, momentum, and energy conservation) are considered, which describe the particle, momentum, and energy conservation. By taking these moments, the Boltzmann equation is reduced to a 3-dimensional, time-dependent problem and describes the plasma in terms of averaged quantities such as density, momentum, and mean energy (Naidis, 2012; Reece Roth, 1995). The heat transfer model aims to predict the thermal behavior in the plasma as well as in the adjacent tissue.. The model combines the thermal energy equation, NavierStokes equations, and Pennes equation inside the tissue (Kurazumi et al., 2008). This is simulated using the heat transfer module in COMSOL.

2.3 Spatial and temporal meshing of the device

The plasma has been discretized on a nite element mesh consisting of triangular elements. The spatial mesh is shown in Fig. 2.

The gas flow rate is fixed at 1 liter per minute for all simulations. Discharge simulations for the pin electrode configuration are time-dependent solution. It is obligatory to define the temporal meshing, so that the time dependent solutions can be performed in four alternation periods.

3 Results and Discussion

3.1 The electron density distribution

The electron density distribution and its behavior are the first item addressed in plasma simulation. As shown in Fig. 3-a, a uniform distribution for the electron density is emerged at zero time. Then, by passing the time, the discharge gradually begins, and the electron density distribution is disrupted. In addition, increase of the electron density begins at the sharp anode, and then it is dragged into the device output by diffusion and fluid velocity (Figs. 3-b to 3-d).

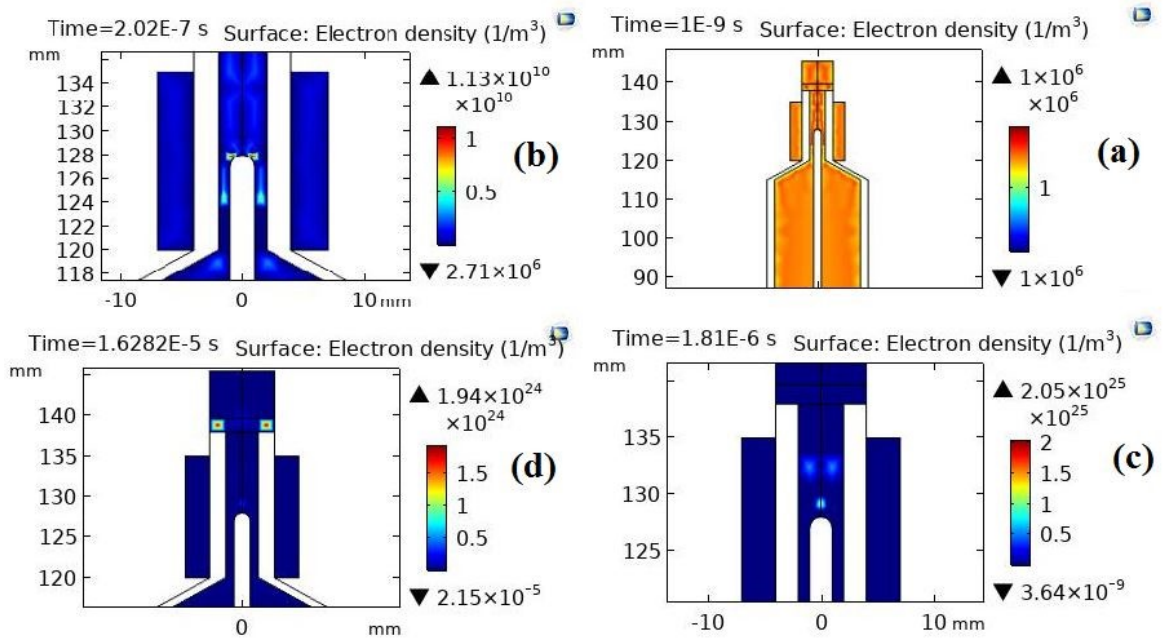

Figure 3: Electron density distribution at different moments: (a) at the starting moment, (b) in a quarter of the period, (c) after half of the period, and (d) in three-quarters of the period.

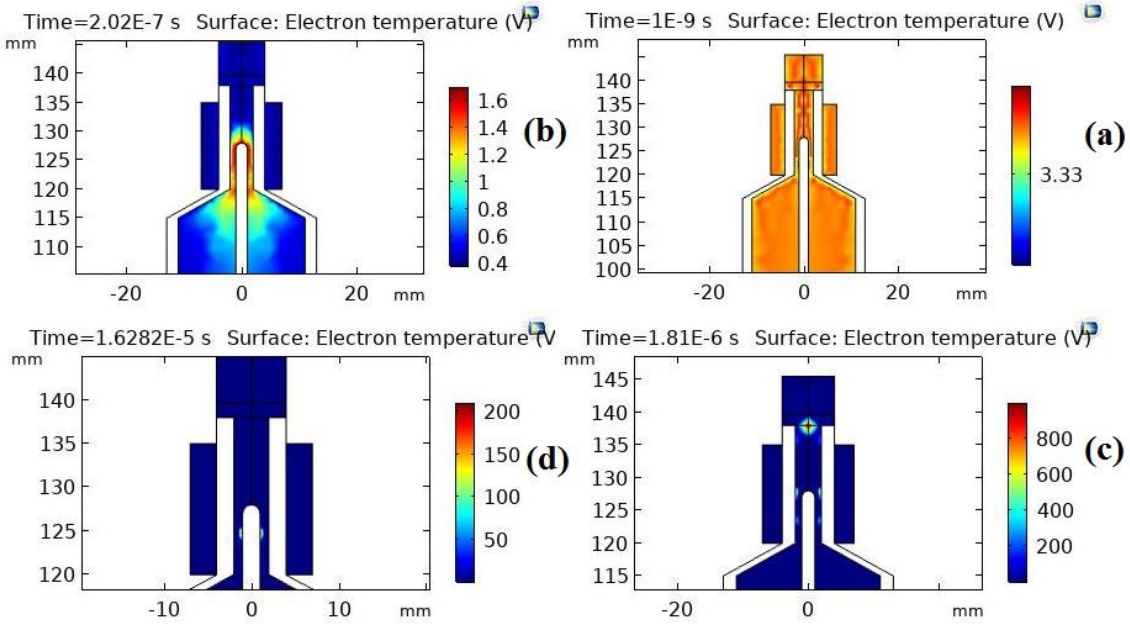

Figure 4: Electron temperature distribution at different moments: (a) at the starting moment, (b) in a quarter of the period, (c) after half of the period, and (d) in three-quarters of the period.

3.2 The electron temperature distribution

The electron temperature is the second most critical factor. Plasma temperature is very important in medical applications, because it determines the tissue temperature and high temperature may damage the tissue. The electron temperature and the gas are balanced by the order of terahertz at atmospheric pressure due to the enormous number of collisions. As a result, the calculation of electron temperature can be a reliable indicator of gaseous temperature in this case. The temperature distribution of the electron is shown in Figs. 4-a to 4-d at various moments when the device is turned on. These jets can emit low temperature plasma plumes in the surrounding air. Because they can maintain temperatures below 40 °C, they can come in touch with biological tissues without causing thermal damage (Laroussi, 2020; Weltmann et al., 2010).

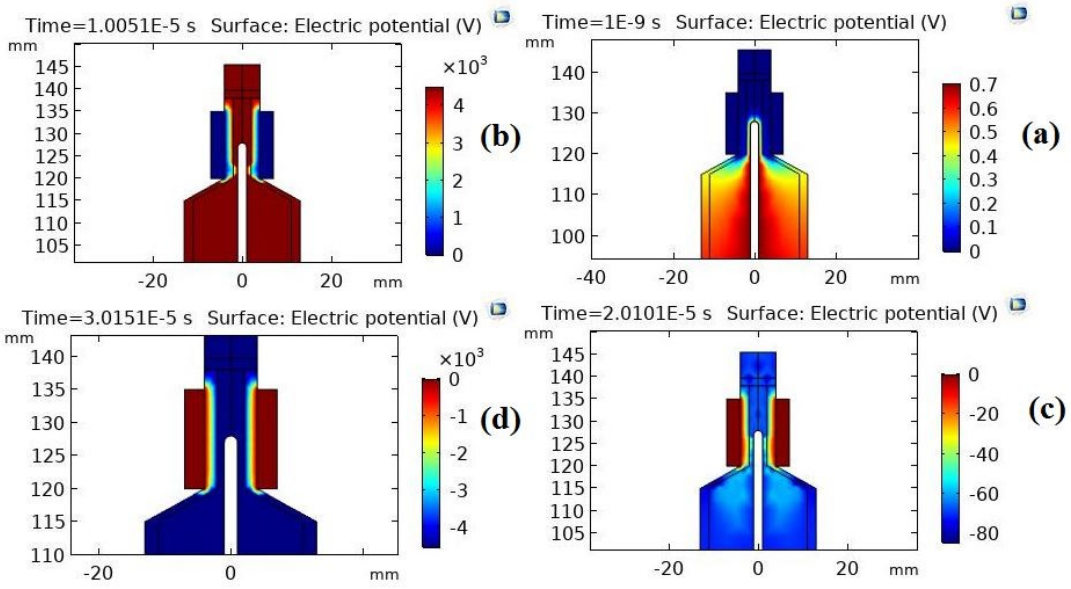

Figure 5: Electrical potential distribution at different moments: (a) at the starting moment, (b) in a quarter of the period, (c) after half of the period, and (d) in three-quarters of the period.

3.3 The electric potential distribution

The spatial distribution of the electric potential is shown in Figs. 5-a to 5-d. The electrical potential over the central electrode as an anode has the largest value and reaches a maximum in a quarter of the period since the applied voltage is sinusoidal. After one-half of the period, on the contrary, the exterior electrode becomes an anode, and the potential difference reaches its maximum value after three-quarters of the period.

4 Conclusions

In this paper, simulation of a typical atmospheric pressure plasma jet using COMSOL Multiphysics was presented. Important plasma parameters such as electron density distribution, temperature distribution, and electric potential were calculated and discussed. The two-dimensional distribution of electron density and temperature at different times were obtained inside the tissue. The average values of the mentioned parameters were calculated about 10^{22} electrons per cubic meter and about 10 volts, respectively. The two-dimensional distribution of the electric potential was also obtained at the times of one-fourth and three-fourths of the period. The results were consistent with the simulations performed by Deepak (Deepak et al., 2018). The electron density obtained by Deepak was of the 10^{16} m^{-3} order and the electron density obtained in this study is of the 10^{16} m^{-3} order at the same time. Effective plasma parameters for treatment were determined by establishing a virtual laboratory before the experiment. The optimization of different variables to attain optimum plasma jet device as the next study is under consideration.

References

Chu, P. K., Chen, J., Wang, L., et al. (2002). Plasma-surface modification of biomaterials. *Materials Science and Engineering: R: Reports*, 36(5-6):143–206.

COMSOL, A. (2018). *Comsol Multiphysics v. 5.4*. www.comsol.com. Stockholm, Sweden. COMSOL AB.

Deepak, G. D., Joshi, N., and Prakash, R. (2018). Model analysis and electrical characterization of atmospheric pressure cold plasma jet in pin electrode configuration. *AIP Advances*, 8(5):055321.

Fridman, G., Friedman, G., Gutsol, A., et al. (2008). Applied plasma medicine. *Plasma Processes and Polymers*, 5(6):503–533.

Hagelaar, G. and Pitchford, L. C. (2005). Solving the Boltzmann equation to obtain electron transport coefficients and rate coefficients for fluid models. *Plasma Sources Science and Technology*, 14(4):722.

Kogelschatz, U., Eliasson, B., and Egli, W. (1997). Dielectric-barrier discharges. principle and applications. *Le Journal de Physique IV*, 7(C4):C4–47.

Kurazumi, Y., Tsuchikawa, T., Ishii, J., et al. (2008). Radiative and convective heat transfer coefficients of the human body in natural convection. *Building and Environment*, 43(12):2142–2153.

Laroussi, M. (2020). Cold plasma in medicine and healthcare: The new frontier in low temperature plasma applications. *Frontiers in Physics*, 8:74.

Lu, X., Naidis, G., Laroussi, M., et al. (2016). Reactive species in non-equilibrium atmospheric-pressure plasmas: Generation, transport, and biological effects. *Physics Reports*, 630:1–84.

Lu, X., Reuter, S., Laroussi, M., and Liu, D. (2019). *Nonequilibrium atmospheric pressure plasma jets: Fundamentals, diagnostics, and medical applications*. CRC Press.

Mazandarani, A., Goudarzi, S., Ghafoorifard, H., et al. (2020). Calculation of temperature and density for dielectric-barrier discharge (DBD) plasma using COMSOL. *Journal of Nuclear Science and Technology (JonSat)*, 40(4):99–108.

Naidis, G. (2012). Modeling of helium plasma jets emerged into ambient air: Influence of applied voltage, jet radius, and helium flow velocity on plasma jet characteristics. *Journal of Applied Physics*, 112(10):103304.

Raizer, Y. P. and Allen, J. E. (1991). *Gas discharge physics*, volume 1. Springer.

Reece Roth, J. (1995). Industrial plasma engineering. *IOP*.

Schröder, M., Ochoa, A., and Breitkopf, C. (2015). Numerical simulation of an atmospheric pressure rf-driven plasma needle and heat transfer to adjacent human skin using COMSOL. *Biointerphases*, 10(2):029508.

Sharma, N. K., Misra, S., Varun, et al. (2020). Experimental and simulation analysis of dielectric barrier discharge based pulsed cold atmospheric pressure plasma jet. *Physics of Plasmas*, 27(11):113502.

Sohbatzadeh, F. and Soltani, H. (2018). Time-dependent one-dimensional simulation of atmospheric dielectric barrier discharge in $N_2/O_2/H_2O$ using comsol multiphysics. *Journal of Theoretical and Applied Physics*, 12(1):53–63.

Weltmann, K. D., Kindel, E., von Woedtke, T., et al. (2010). Atmospheric-pressure plasma sources: Prospective tools for plasma medicine. *Pure and Applied Chemistry*, 82(6):1223–1237.

Yan, D., Sherman, J. H., and Keidar, M. (2017). Cold atmospheric plasma, a novel promising anti-cancer treatment modality. *Oncotarget*, 8(9):15977.